

# Controlled electrophoretic deposition of electrochemically exfoliated graphene sheets on Ag nanowires network

Mahdi Malekshahi Byranvand<sup>1</sup> ✉, Fariba Tajabadi<sup>2</sup>, Saeed Mardi<sup>1</sup>, Nima Taghavinia<sup>1,3</sup>, Ali Amiri Zarandi<sup>4</sup>, Ali Dabirian<sup>5</sup>

<sup>1</sup>Physics Department, Sharif University of Technology, Tehran, Iran

<sup>2</sup>Department of Nanotechnology and Advanced Materials, Materials and Energy Research Center, Karaj, 31787-316, Iran

<sup>3</sup>Institute for Nanoscience and Nanotechnology, Sharif University of Technology, Tehran, Iran

<sup>4</sup>Polymer & Color Engineering Department, Amir Kabir University of Technology, Tehran, Iran

<sup>5</sup>Institute for Research in Fundamental Sciences, School of Physics, Tehran, Iran

✉ E-mail: Mahdi.malekshahi@gmail.com

Published in Micro & Nano Letters; Received on 23rd April 2018; Revised on 30th October 2018; Accepted on 7th December 2018

Electrochemical exfoliation of graphite has recently attracted a big attention as a simple, fast and scalable method for the preparation of high quality graphene, but there are some drawbacks that hinder its application. Direct deposition is one of the most critical challenges that makes it difficult to deposit uniform, compact and large scale graphene thin films. This work develops a facile electrophoretic deposition route to fabricate exfoliated graphene (EG) film on Ag nanowires (NWs) networks with a controllable film thickness in nanometers scale. EG thin films are deposited with different applied potentials and times from an EG dispersion in *N*, *N*-dimethylformamide solvent. Since confirmed by light transmittance results, the increase in deposition time or applied potential lead to an increase in the number of deposited EG layers. The scanning electron microscopy results confirm the uniformity and compactness of EG films deposited on Ag NWs network. Furthermore, transparency and conductivity of Ag NWs films before and after the deposition of EG are investigated. It shows significant improvement in its performance, as a result, it leads to Ag NWs/EG hybrid films exhibiting a sheet resistance of  $R_s = 30 \Omega \text{ sq}^{-1}$ , and 85% light transmittance, comparable to conventional transparent conductive oxide films.

**1. Introduction:** Electrochemical exfoliation of graphite has drawn increasing attention over the last few years. It has the potential to prepare high-quality graphene in large-scale under mild conditions. This method is simple and fast compared to other synthesis methods. Generally, electrochemical approaches to the preparation of graphene materials involve the use of an electrolyte, and an electrical current to induce structural deformation of a graphite working electrode, either via cathodic reduction or anodic oxidation of the graphite source electrode [1–7]. The working electrode is a graphite rod/film or highly orientated pyrolytic graphite sample. This method holds enormous promise as a simple, green and high-yield method for the mass production of single- and few-layer flakes of a structural quality better than that of reduced graphene oxide (RGO) [1–7].

Self-assembly of electrochemically exfoliated graphite into electrochemically exfoliated graphene (EG) sheets requires the dispersion of electrochemically exfoliated graphite in a solvent with strong interface interactions between EG and the functional groups of solvents. Due to its hydrophobic nature and low oxide content, EG very well disperses in polar aprotic solvents with a high boiling point; e.g. *N*, *N*-dimethylformamide (DMF) and *N*-methyl-2-pyrrolidone. Unfortunately, it creates a major obstacle for solution processing and the self-assembly of EG [7–9]. This makes it difficult to employ conventional solution processing techniques for thin film preparation, such as spin-coating, inkjet-printing, rod-coating, and/or layer-by-layer deposition.

There have been several reports on the deposition of EG sheets. For examples, Parvez *et al.* have reported coating commercial A4-size substrates by EG dispersion in DMF using a paintbrush [9]. Spray deposition has also been used for deposition of EG/Poly(3,4-ethylenedioxythiophene)-poly(styrenesulfonate) (PEDOT:PSS) dispersion in DMF for transparent conductive film (TCF) fabrication [10]. Marković *et al.* used the electrochemical EG sheets dispersed in DMF for fabrication of semi-TCFs on a glass ceramic substrate by a two-step method; deposition of EG

on ano-discs by vacuum filtration and then transferred to glass ceramic substrates [11]. However, the development of an easy and fast method for deposition of EG on different substrates is an important challenge.

Among various deposition methods for carbon nanostructures, the electrophoretic deposition (EPD) method is a well-developed and economical method that has been successfully applied for the deposition of carbon nanostructures including nanotubes [12], graphene oxide (GO) [13–15] and RGO [16–18], on different conductive substrates. It enjoys a number of advantages in preparation of thin films from charged colloidal suspensions, including a high deposition rate, good thickness controllability, good uniformity, and scalability [19]. EPD leads to RGO or GO uniform films with good surface coverage at a relatively high thickness (hundred nanometres or micrometres scale). However, RGO or GO films with well-defined coverage deposited in nm scales. Here we report deposition of electrochemically EG by the EPD method on Ag nanowires (Ag NWs) network with a controlled film thickness in nm scale without any additive or addition reduction process. However, as described previously [20] due to the holes in the film, the Ag NWs network needs an overlayer to fill non-conductive empty spaces between NWs. In addition, the overlayer can decrease film surface roughness and also improve Ag NWs adhesion to the substrate. Also, EG deposition on the cross junctions of Ag NWs leads to bridging the charge transport across adjacent Ag NWs and lowering  $R_s$  of the Ag NWs network [20].

The graphene deposition is carried out within the timescale of a few minutes. The graphene percolation significantly enhanced electrical properties such as low sheet resistance with a negligible decrease of optical transparency. In comparison with another method, our fabrication method is so easy without any additional reaction and pre- or post-treatments. Final graphene/Ag NWs hybrid films show  $T = 52\%$  (at 550 nm) and  $R_s = 30 \Omega \text{ sq}^{-1}$ , which is comparable to conventional TCO films.

## 2. Material and methods

**2.1. EG synthesis:** EG was synthesised following a published procedure [9]. A graphite foil (Alfa Aesar) was used as an anode and a Pt wire was used as a cathode for electrochemical exfoliation of graphite in 0.1 M  $(\text{NH}_4)_2\text{SO}_4$  aqueous electrolyte. The distance between the graphite foil and the Pt electrode was 2 cm and was kept constant throughout the electrochemical process. Electrochemical exfoliation was carried out by applying a positive voltage (10 V) between the two electrodes. After the graphite exfoliation was completed, the product was collected through a polytetrafluoroethylene (PTFE) membrane filter with 0.2  $\mu\text{m}$  pore size and washed several times with de-ionised (DI) water followed by vacuum filtration. The wetted resultant EG powder was then dispersed in DMF (2 mg  $\text{ml}^{-1}$ ) by sonication at a low power for 10 min.

**2.2. Synthesis and deposition of Ag NWs:** Ag NWs film was prepared by dip-coating of Ag NW on a glass substrate. The ethanolic solution of Ag NWs with 5 mg/ml was prepared as reported previously [20]. The dip-coating process was done with a home-made dip coater at a rate of 6  $\text{mm s}^{-1}$ .

**2.3. Deposition of EG sheets Ag NWs network by EPD method:** An EG dispersion in DMF was used for EPD. The Ag NWs network film was used as the anode for deposition of EG at positive potentials. For deposition of EG on Ag NWs network, a potential of 6 V with 1 mg/ml concentration (EG in DMF) was used.

**2.4. Physical characterisations:** The morphology and surface were investigated by using a field-emission scanning electron microscope (TESCAN, Mira 3-XMU) and atomic force microscopy (AFM) (VEECO-CP Research). The contact angles were measured by an optical contact angle (OCA) 15 plus and chemical structures of samples were studied by Fourier transform infrared (FTIR) spectra (Shimadzu-8400S spectrometer) and X-ray photoelectron spectroscopy (XPS) (VGICROTECH, X-ray 8025-Bestec). The optical transmittance and absorbance of the TCFs were measured with an ultraviolet–visible spectrophotometer (Avaspec 2048-TEC) using an integrating sphere.

## 3. Results and discussions

**3.1. XPS, Fourier transform-infrared (FT-IR) and AFM analysis of EG sheets:** X-ray photo-electron spectroscopy (XPS), FT-IR spectroscopy and AFM were employed for characterisation of EG. The high-resolution C 1s XPS spectrum of the EG sheets (Fig. 1a) shows a sharp peak at 284.5 eV that corresponds to C–C bonds of carbon atoms in a conjugated honeycomb lattice. Peaks at 285.5, 287.6 and 290.1 eV could be attributed to different C–O bonding configurations due to the oxidation and destruction of the  $\text{sp}^2$  atomic structure of graphite as reported previously [21, 22].

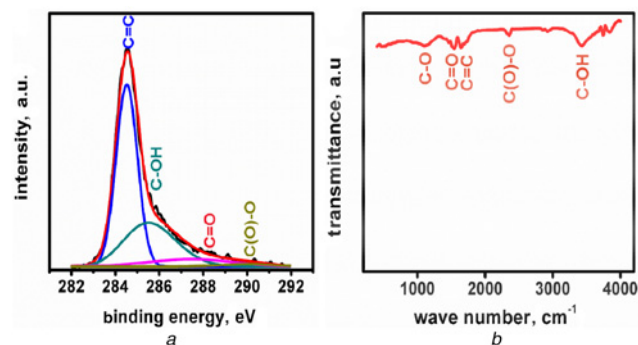


**Fig. 1** EG characterisation with  
a Peak fitted C 1s XPS spectra of EG  
b FTIR spectrum of EG sheets

The percentage proportion of different carbon environments in C 1s was 68.8, 22.3, 8.8, and 0.1% corresponding to the C=C, C–OH, C=O and C(O)–O, respectively. As expected, the relative percentage of C=C bonds is significantly higher than the carbon oxide content similar to RGO. Fig. 1b shows the FTIR spectrum for EG sheets. The peak at  $1650\text{ cm}^{-1}$  indicates skeletal vibrations from un-oxidised graphitic domains ( $\text{--C=C--}$ ) as is reported for RGO. The peaks at  $3410\text{--}3440$ ,  $1400\text{--}1500$ , and  $1050\text{ cm}^{-1}$  indicate the presence of C–OH, C=O, and C–O stretching vibrations in the EG, respectively. The AFM image (Fig. S1) shows single-layer EG sheets. Zeta potential measurement showed that the EG dispersion has a negative potential as high as  $-28 \pm 4\text{ mV}$ . This negative potential can result from different oxide groups C–OH, C(O)–O and C–O in EG as confirmed by XPS and FT-IR analysis (Fig. 1). Previous studies for EG dispersion in DMF showed a negative zeta potential of about  $-21\text{ mV}$  [23]. The fairly high zeta potential provides electrostatic repulsion among the colloidal sheets, similar to the colloidal behaviour of GO in aqueous solution [24]. It is important to notice that the zeta potential value is lower than that reported for GO (usually  $>40\text{ mV}$  depending on pH and oxidation degree) [25].

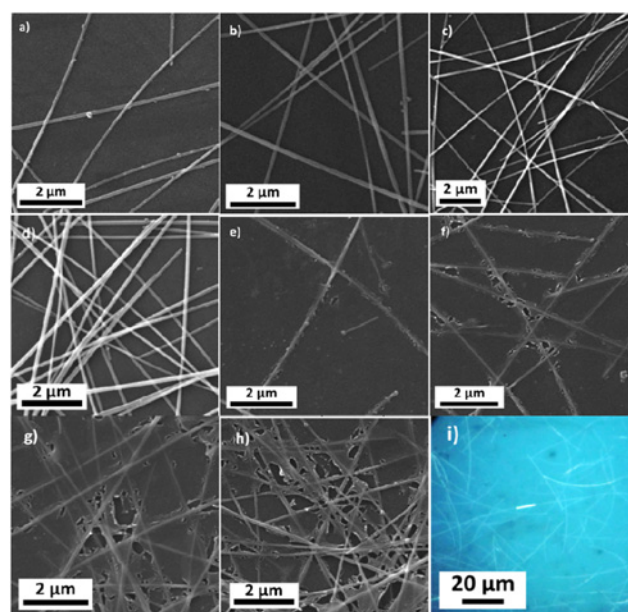


**Fig. 2** SEM pictures of Ag NWs with  
a one-step  
b two-step  
c three-step  
d five-step dip-coating and after EG deposition at 6 V for 30 s  
e, f, g, h, i Optical microscopy image of Ag NWs deposited on the glass substrate

**Table 1** Sheet resistance variations of Ag NWs film (0–5 steps dip-coating) after deposition of EG at a deposition potential of 6 V for 0, 30, 60 and 120 s

Dip coating steps	Sheet resistance ( $\Omega\text{ sq}^{-1}$ )			
	0 s	30 s	60 s	120 s
1	850,000	10,000	5000	500
2	140	70	75	78
3	85	30	40	52
5	22	12	17	18
7	19	11	13	20

3.2. EG deposition on Ag NWs network: Figs. 2a–d show scanning electron microscopy (SEM) images of Ag NW films with one-, two-, three- and five-step dip coating on glass substrates,

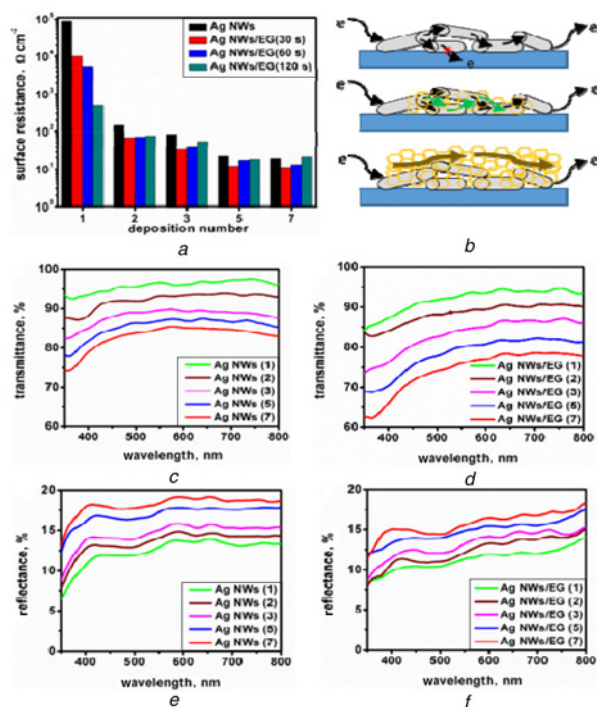


**Fig. 3** Transparent conductive film

a Sheet resistance variations of Ag NWs films (0–7 steps dip-coating) before and after deposition of EG at a deposition potential of 6 V for 0, 30, 60 and 120 s  
b Schematic of electron transport on Ag NWs and Ag NWs/EG film and effect of thickness of graphene layer  
c Optical transmittance of Ag NWs films at different dip-coating steps  
d After EG deposition at 6 V for 30 s  
e Diffuse reflectance spectra of Ag NWs films at different dip-coating steps  
f After EG deposition at 6 V for 30 s

respectively. As mentioned in the experimental part, the dip coating method was used for the deposition of Ag NWs on glass substrates. Successive dip coatings lead to a higher density of Ag NWs on the substrate surface and lower light transmission. The SEM images demonstrate that a randomly cross-linked Ag NWs network is built on the substrate surface with a very low coverage ratio at one- and two-step dip coating permitting high light transmittance. As is expected, higher dip coating steps lead to the higher density of Ag NWs on the substrate surface. As is clearly shown in Figs. 2e–h, the EG sheets effectively cover the Ag NWs and the empty spaces between NWs.

3.3. Properties of TCFs: Table 1 and Fig. 3a display sheet resistance variations of Ag NWs film before and after deposition of EG at a deposition potential of 6 V for 30, 60 and 120 s. The film resistance measurement was not reproducible for a lower amount of potential ( $E < 6$  V). As can be seen in this Figure the sheet resistance dramatically decreases for Ag NWs film deposited by one-step dip coating; it decreases from  $85 \text{ k}\Omega \text{ sq}^{-1}$  to 10, 5 and  $0.6 \text{ k}\Omega \text{ sq}^{-1}$  for 30, 60 and 120 s deposition time. The significant decrease in resistance of Ag NWs film with graphene deposition can be mostly due to the covering of the non-conductive large empty spaces between Ag NWs with conductive EG. As can be seen in Fig. 2a, the space between Ag NWs is large and graphene sheets connect them and that is why it shows this significant improvement. Other Ag NWs films with a higher density of Ag NWs (two-, three-, five- and seven-step-dip coating) show a moderate decrease in surface resistance with 30 s deposition of EG while with increasing deposition time their resistance increase. This mechanism is shown in Fig. 3b, how the increase of deposition time can have an effect on flowing current through the electrode, increasing conductivity with EG coating in short deposition time (about 30 s) can be ascribed to the improvement in electrical contact quality in the Ag NWs network since the average spacing between the overlapping Ag NWs is decreased after EG coating. However as expected for longer EG deposition time, a higher amount of EG can be deposited, and as is shown in Fig. 1a due to the presence of different oxide groups in EG, high amount of EG sheets can lead to more junction resistance between EG

**Table 2** Comparison of transmittance and conductivity of Ag NW/EG TCFs with previously reported results

	Ag NWs coating methods	Graphene synthesis and coating methods	Treatments	T, %	Conductivity, $\Omega/\text{cm}^2$	Ref
Ag NWs/G	drop casting	chemical vapour deposition (CVD) method	CVD grown graphene on Cu substrate, etching and transferring to a quartz substrate, Ag NWs drop casting, thermal annealing 300°C for 1 h	88	22	[28]
Ag NWs/ZnO:F	spin coating	pulsed laser deposition	Ag NWs were applied by plasma cleaning to eliminate the Polyvinylpyrrolidone (PVP) adhering to the surface of the Ag NWs	83	17.5	[29]
graphene/Ag NWs	spin coating	CVD	etching of Cu and transferring by Poly(methyl methacrylate) (PMMA) polymer on to Ag NWs surface	81.5	32.5	[24]
Ag NWs/RGO-NH <sup>3+</sup>	Meyer rod coating	Spray	GO-NH <sup>3+</sup> suspension was prepared by reaction of GO with <i>N</i> -ethyl- <i>N'</i> -(3-dimethyl amino propyl) carbodiimide methiodide and ethylenediamine. GO-NH <sup>3+</sup> suspensions were reduced using a hydrazine solution.	89	18.2	[30]
Ag NWs/p-RGO	wire wound coating	—	one-step preparation of Ag NWs/p-RGO by polyol method, too long synthesis time (>48 h)	94.6	25	[31]
PEDOT:PSS/Ag NWs/graphene	spin coating	spin coating	thermal annealing at 120, 100, and 150°C for each layer, respectively	83	223	[32]
RGO/Cu–Ag NWs	bar coating	dip-coating	GO was reduced by hydrazine solution	77.6	10	[33]
Ag NWs/GO	bar coating	spray	plasma surface treatment	90	30	[34]
Ag NWs/EG	dip coating	electrophoretic	drying for 2 min at 100°C after EG deposition	85	30	This work



sheets and Ag NWs and electrical current mostly flows through the EG sheet. For these reasons, 30 s was chosen as the optimised deposition time for further studies.

The optical transmittance spectra of the different Ag NWs films before and after deposition of EG for 30 s are shown in Figs. 3c and d, respectively. As is expected, Ag NWs films transmittance decreases with increasing dip coating steps that can be explained by increasing Ag NWs density on the substrate surface.

The optical transmittance is 96.6% at 550 nm for Ag NWs film with one-step dip coating step and decreases to 93.2, 88.5, 86.5 and 84.8% for two-, three-, five- and seven-step dip coating. The hybrid films show a value of 4–11% decrease in transmittance after deposition of EG sheets on the Ag NWs film that is due to light absorption by few layer graphene coating. It is well-known that a CVD-grown monolayer graphene absorbs about 2.3% of visible light [26, 27]. It is valuable to note the transmittance decline is lesser for low density Ag NWs films (one- and two-step dip coating) compared with higher density one. A high density of Ag NWs can attract more EG sheets during EPD than low density one in the same time. The latter result is probably due to the relation between conductivity and coverage of Ag NWs films with a deposition rate of EG sheets on the substrate.

Fig. S2 shows the transmittances of different electrodes after EG deposition at 550 nm with the surface electrical resistances of Ag NW/EG in terms of different dip coating steps. When the dip coating step increased from 1 to 2, 3, 5, and 7 min, the surface resistances of Ag NW/EG TCFs decreased significantly. However, the transparency of Ag NW/EG TCFs also decreased obviously. The electrode with three steps showed 30  $\Omega$ /sq surface resistance and high 85% transmittance which is comparable to commercial TCO films. Consequently, this electrode was chosen as the optimal electrode for preparing high performance TCFs.

Figs. 3e and f show the diffused reflectance spectra of Ag NWs and EG/Ag NWs films. The reflection of Ag NWs films decreases by about 2–3% after coating of Ag NWs with EG sheets as shown in this figure. The decrease in diffuse reflectance indicates the film is becoming more planar and smooth. Compared with a similar reported article for Ag NWs/graphene (GO), EPD of EG on Ag NWs network is very fast (30 s) and easy and without any additional reaction or treatment. Moreover, the properties of the final transparent film were compared in Table 2 with some reports in recent years. It clearly shows that Ag NW/EG TCFs have good performance compared with transparent conductive based on graphene and GO.

**4. Conclusion:** Our results show the electrophoresis method can be used as a fast and easy method for deposition of EG on Ag NWs surface as a model conductive substrate. The graphene sheets deposition on a network of Ag NWs leads to Ag/NWs graphene hybrid films which in the EG sheets effectively cover the Ag NWs and the empty spaces between NWs. The graphene percolation significantly enhanced the electrical properties such as low sheet resistance with negligible degradation of optical transparency.

## 5 References

- [1] Low C.T.J., Walsh F.C., Chakrabarti M.H., *ET AL.*: 'Electrochemical approaches to the production of graphene flakes and their potential applications', *Carbon*, 2013, **54**, pp. 1–21
- [2] Abdelkader A.M., Kinloch I.A., Dryfe R.A.W.: 'Continuous electrochemical exfoliation of micrometer-sized graphene using synergistic ion intercalations and organic solvents', *ACS Appl. Mater. Interfaces*, 2014, **6**, pp. 1632–1639
- [3] Wu L., Li W., Li P., *ET AL.*: 'Powder, paper and foam of few-layer graphene prepared in high yield by electrochemical intercalation exfoliation of expanded graphite', *Small*, 2014, **10**, pp. 1421–1429
- [4] Rao K.S., Senthilnathan J., Liu Y.-F., *ET AL.*: 'Role of peroxide ions in formation of graphene nanosheets by electrochemical exfoliation of graphite', *Sci. Rep.*, 2014, **4**, p. 4237
- [5] Wang J., Manga K.K., Bao Q., *ET AL.*: 'High-yield synthesis of few-layer graphene flakes through electrochemical expansion of graphite in propylene carbonate electrolyte', *J. Am. Chem. Soc.*, 2011, **133**, pp. 8888–8891
- [6] Su C.Y., Lu A.-Y., Xu Y., *ET AL.*: 'High-quality thin graphene films from fast electrochemical exfoliation', *ACS Nano*, 2011, **5**, pp. 2332–2339
- [7] Parvez K., Li R., Puniredd S.R., *ET AL.*: 'Multiwall nanotubes, multi-layers, and hybrid nanostructures: new frontiers for technology and Raman spectroscopy', *ACS Nano*, 2013, **7**, pp. 3598–5606
- [8] Yang S., Lohe M.R., Müllen K., *ET AL.*: 'New-generation graphene from electrochemical approaches: production and applications', *Adv. Mater.*, 2016, **28**, pp. 6213–6221
- [9] Parvez K., Wu Z.-S., Li R., *ET AL.*: 'Exfoliation of graphite into graphene in aqueous solutions of inorganic salts', *J. Am. Chem. Soc.*, 2014, **136**, pp. 6083–6091
- [10] Liu Z., Parvez K., Li R., *ET AL.*: 'Transparent conductive electrodes from graphene/PEDOT:PSS hybrid inks for ultrathin organic photo-detectors', *Adv. Mater.*, 2015, **27**, pp. 669–675
- [11] Marković Z.M., Budimir M.D., Kepić D.P., *ET AL.*: 'Semi-transparent, conductive thin films of electrochemically exfoliated graphene', *RSC Adv.*, 2016, **6**, pp. 39275–39283
- [12] Boccaccini A.R., Cho J., Roether J.A., *ET AL.*: 'Electrophoretic deposition of carbon nanotubes', *Carbon*, 2006, **44**, pp. 3149–3160
- [13] Chavez-Valdez A., Shaffer M.S.P., Boccaccini A.R.: 'Applications of graphene electrophoretic deposition. A review', *J. Phys. Chem. B*, 2012, **117**, pp. 1502–1515
- [14] Wang M., Duong L.D., Oh J.-S., *ET AL.*: 'Large-area, conductive and flexible reduced graphene oxide (RGO) membrane fabricated by electrophoretic deposition (EPD)', *ACS Appl. Mater. Interfaces*, 2014, **6**, pp. 1747–1753
- [15] Deng C., Jiang J., Liu F., *ET AL.*: 'Influence of graphene oxide coatings on carbon fiber by ultrasonically assisted electrophoretic deposition on its composite interfacial property', *Surf. Coatings Technol.*, 2015, **272**, pp. 176–181
- [16] Zhang H., Zhang X., Zhang D., *ET AL.*: 'One-step electrophoretic deposition of reduced graphene oxide and Ni(OH)<sub>2</sub> composite films for controlled syntheses supercapacitor electrodes', *J. Phys. Chem. B*, 2013, **117**, pp. 1616–1627
- [17] Diba M., Fam D.W.H., Boccaccini A.R., *ET AL.*: 'Electrophoretic deposition of graphene-related materials: A review of the fundamentals', *Prog. Mater. Sci.*, 2016, **82**, pp. 83–117
- [18] Wang Q., Vasilescu A.M., Wang Q., *ET AL.*: 'Electrophoretic approach for the simultaneous deposition and functionalization of reduced graphene oxide nanosheets with diazonium compounds: application for lysozyme sensing in serum', *ACS Appl. Mater. Interfaces*, 2017, **9**, pp. 12823–12831
- [19] Ye L., Wen K., Zhang Z., *ET AL.*: 'Highly efficient materials assembly via electrophoretic deposition for electrochemical energy conversion and storage devices', *Adv. Energy Mater.*, 2016, **6**, p. 150218
- [20] Hu L., Kim H.S., Lee J.-Y., *ET AL.*: 'Scalable coating and properties of transparent, flexible, silver nanowire electrodes', *ACS Nano*, 2010, **4**, pp. 2955–2963
- [21] Some S., Ho S.-M., Dua P., *ET AL.*: 'Dual functions of highly potent graphene derivative-poly-L-lysine composites to inhibit bacteria and support human cells', *ACS Nano*, 2012, **6**, pp. 7151–7161
- [22] Park S., An J., Jung I., *ET AL.*: 'Colloidal suspensions of highly reduced graphene oxide in a wide variety of organic solvents', *Nano Lett.*, 2009, **9**, pp. 1593–1597
- [23] Wei W., Wang G., Yang S., *ET AL.*: 'Efficient coupling of nanoparticles to electrochemically exfoliated graphene', *J. Am. Chem. Soc.*, 2015, **137**, pp. 5576–5581
- [24] Liu Y., Chang Q., Huang L.: 'Transparent, flexible conducting graphene hybrid films with a subpercolating network of silver nanowires', *J. Mater. Chem. C*, 2013, **1**, pp. 2970–2974
- [25] Krishnamoorthy K., Veerapandian M., Yun K., *ET AL.*: 'The chemical and structural analysis of graphene oxide with different degrees of oxidation', *Carbon. N. Y.*, 2013, **53**, pp. 38–49
- [26] Kuzmenko A.B., Van Heumen E., Carbone F., *ET AL.*: 'Universal optical conductance of graphite', *Phys. Rev. Lett.*, 2008, **100**, p. 117401
- [27] Nair R.R., Blake P., Grigorenko A.N., *ET AL.*: 'Fine structure constant defines visual transparency of graphene', *Science*, 2008, **320**, p. 1308
- [28] Chen R., Das S.R., Jeong C., *ET AL.*: 'Co-percolating graphene-wrapped silver nanowire network for high performance, highly stable, transparent conducting electrodes', *Adv. Funct. Mater.*, 2013, **23**, pp. 5150–5158

- [29] Han J., Yuan S., Liu L., *ET AL.*: 'Fully indium-free flexible Ag nano-wires/ZnO:F composite transparent conductive electrodes with high haze', *J. Mater. Chem. A*, 2015, **3**, pp. 5375–5384
- [30] Sun Q., Lee S.J., Kang H., *ET AL.*: 'Positively-charged reduced graphene oxide as an adhesion promoter for preparing a highly-stable silver nanowire film', *Nanoscale*, 2015, **7**, pp. 6798–6804
- [31] Lai Y.-T., Tai N.-H.: 'One-step process for high-performance, adhesive, flexible transparent conductive films based on p-type reduced graphene oxides and silver nanowires', *ACS Appl. Mater. Interfaces.*, 2015, **7**, pp. 18553–18559
- [32] Altin Y., Tas M., Borazan I., *ET AL.*: 'Enhancement of transparent conductive electrodes for third generation photovoltaics', *Surf. Coatings Technol.*, 2016, **302**, pp. 75–81
- [33] Kim J., Lim J.W., Mota F.M., *ET AL.*: 'Reduced graphene oxide wrapped core-shell metal nanowires as promising flexible transparent conductive electrodes with enhanced stability', *Nanoscale*, 2016, **8**, pp. 18938–18944
- [34] Moon I.K., Kim J.I., Lee H., *ET AL.*: '2D graphene oxide nanosheets as an adhesive over-coating layer for flexible transparent conductive electrodes', *Sci. Rep.*, 2013, **3**, p. 1112